

# **EUROFEL-Report-2007-DS2-084 c**

## *EUROPEAN FEL Design Study*



Deliverable N°: D 2.11


Deliverable Title: Wakefield effects studied by simulations and experiments - IMAGE CURRENT HEATING OF THE 4GLS NARROW GAP VESSELS AND COLLIMATORS

Task: DS-2

Authors: see next page

Contract N°: 011935

**Project funded by the European Community  
under the “Structuring the European Research Area” Specific Programme  
Research Infrastructures action**

		fgls-desn-rpt-022 Date: September 2007
---	--	---

## IMAGE CURRENT HEATING OF THE 4GLS NARROW GAP VESSELS AND COLLIMATORS

*Duncan Scott*

*ASTeC  
Daresbury Laboratory  
Warrington WA4 4AD  
United Kingdom*

### **Abstract**

The fields of the bunches in an accelerator induce image currents in the vacuum vessel walls. Due to the non-zero resistance of the vessel walls these image currents dissipate power in the form of heat in the vessel. The effect is known as *resistive wall heating*. Calculations of the resistive wall heating for different bunch lengths and vessel apertures in the normal conducting and anomalous skin effect regimes are presented. The results show that the heating of the High Average Current Loop (HACL) is  $\sim \text{kW m}^{-1}$  for the shortest bunch lengths. There is  $\sim 50 \text{ Wm}^{-1}$  of heating at the HACL collimators and this could have an impact on the engineering design. Installing a vessel at cryogenic temperatures is probably not feasible in the 4GLS HACL. The amount of heating means that the room temperature permanent magnet undulators will require cooling to maintain their magnetic performance. This could result in a increase in the minimum magnetic gap. The heating of the XUV-FEL line vessels is  $\sim \text{W m}^{-1}$  and assumed to be negligible.

*Responsible Author: Duncan Scott*

*Authorised By: Jim Clarke*

## 1. Introduction

In general, when a longitudinal charge distribution traverses an impedance it can lose energy to that impedance. For a resistive wall impedance, the amount of energy lost can be found by considering the heating of the vessel due to image currents induced by the beam or by considering the energy lost by the beam due to resistive wall wakefields. Both should be ideally the same. In 4GLS there are narrow gap vessels for the undulator modules and collimators and these will receive the most beam heating. In order to ensure the heating is not too great for the operation of the undulators and collimators it needs to be calculated.

Equivalent sets of equations for calculating the heating due to image currents have been derived to describe the effect in the LHC dipoles [1, 2] and also for a number of different superconducting planar undulators considered for light sources, [3, 4, 5, 6]. To calculate the power dissipated in a conducting vessel due to the image currents the surface resistance,  $R_s$ , of the vessel must be accurately modelled. The correct model to use depends on factors such as: the temperature of the metal,  $T$ , the frequency of the applied field,  $\omega$ , and the magnitude of any external magnetic field,  $B$ . The total power dissipated due to resistive wall heating,  $P_T$ , in  $\text{W m}^{-1}$ , from Gaussian bunches with rms bunch length,  $\sigma_b$ , in a circular vessel of radius,  $r$ , and surface resistance,  $R_s(\omega)$ , is [4]:

$$P_T = \sum_{n=0}^{\infty} P_{s,n} ,$$

$$P_{s,0} = \frac{1}{2\pi} R_s(0) I_0^2 ,$$

$$P_{s,n} = \frac{1}{2\pi} R_s(0) 2I_0^2 \text{Exp} \left[ - \left( \frac{n\sigma_b \omega_0}{c} \right)^2 \right] ,$$

where  $\omega_0$  is  $2\pi$  divided by the bunch spacing in seconds,  $I_0$  is the time averaged current and  $c$  is the speed of light.

### $R_s$ in the Normal Conducting Regime

In the normal conducting regime, for example at room temperature, the surface resistance,  $R_{s,\text{normal}}$  is:

$$R_{s,\text{normal}} = \sqrt{\frac{\omega \mu_0 \rho}{2}} ,$$

where  $\mu_0$  is the vacuum permeability and  $\rho$  is the DC resistivity of the vessel. In this regime the field penetrates into the metal a certain distance given by the skin depth,  $\delta_{sk}$ :

$$\delta_{sk} = \sqrt{\frac{2\rho}{\omega \mu_0}} .$$

## Residual Resistance Ratio and Magneto-Resistance

If the vessel is cooled to cryogenic temperatures then the resistivity decreases by a factor determined by its residual resistance ratio, RRR, to give a temperature dependant resistivity,  $\rho_T$ :

$$\rho_T = \frac{\rho}{RRR}.$$

Magneto-resistance is when the conductivity of a material is limited by an external magnetic field. Magneto-resistance is an affect seen in high purity metals, with a high RRR value, operating at low temperatures and in high magnetic fields. The resistivity of the material,  $\rho_{BT}$ , is determined by Kohler's rule [7]:

$$\rho_{BT} = \rho_T \left( 1 + 10^{1.055 \text{Log}_{10}(B.RRR) - 2.69} \right).$$

## $R_s$ in the Anomalous Skin Effect Regime

As the resistivity decreases the mean free path between collisions of the conduction electrons,  $\lambda$ , can eventually become greater than  $\delta_{sk}$  and only the fraction of conduction electrons moving parallel to the metal surface are effective in carrying current. The classical theory of conductivity breaks down and the theory of the anomalous skin effect (ASE) must be used [8]. In the ASE theory the surface resistance,  $R_{s,anom}$ , is [9]:

$$\begin{aligned} R_{s,anom} &= R_\infty (1 + 1.157 \alpha^{-0.276}), \\ \alpha &= \frac{3}{4} \omega \mu_0 (\rho_{BT} \lambda)^2 \rho_{BT}^{-3}, \\ R_\infty &= \left[ \frac{\sqrt{3}}{16\pi} \rho_{BT} \lambda (\omega \mu_0)^2 \right]^{\frac{1}{3}}. \end{aligned}$$

## 2. Beam Properties

The relevant beam properties for 4GLS are given in Table 1. The High Average Current Loop (HACL) and the XUV-FEL line have been considered. The beam properties are considerably different for each line.

Parameter	Unit	HACL	XUV-FEL
$I_0$	A	0.1	$1 \cdot 10^{-6}$
Peak Bunch frequency	Hz	$1.3 \cdot 10^9$	$1 \cdot 10^3$
Electrons per bunch		$4.8 \cdot 10^8$	$6.25 \cdot 10^9$
rms Bunch Length	fs	50 - 1000	50 - 1000

Table 1: relevant 4GLS beam parameters.

### 3. Vessel Properties

4GLS currently uses vessels made of aluminium as it has the least effect on the beam energy spread [10, 11]. However in reality an aluminium alloy will be used. There is also the possibility of using copper, or a copper coated vessel, therefore all three of these materials have been considered. The values for the conductivity and  $\rho_{BT}\lambda$  for bulk copper, aluminium and an aluminium alloy type 6164 are given in Table 2. Values of  $\lambda$  for the aluminium alloy are difficult to find (although they could be measured experimentally if needed) and so the bulk aluminium values have been used in the following analysis.

	$\sigma_c(300K)$	$\lambda(300K)$	$\rho_{BT}\lambda$
Unit	$(\Omega m)^{-1}$	$m$	$\Omega m^2$
Copper	$5.9 \cdot 10^7$	$4.2 \cdot 10^{-8}$	$6.6 \cdot 10^{-16}$
Aluminium (pure)	$3.6 \cdot 10^7$	$1.6 \cdot 10^{-8}$	$4.5 \cdot 10^{-16}$
Aluminium Type 6164	$2.3 \cdot 10^7$	$1.6 \cdot 10^{-8}$	$4.5 \cdot 10^{-16}$

Table 2: conductivity and mean free path of conduction electrons for bulk copper and aluminium and an aluminium alloy at 300K.

The vessels in 4GLS will have a range of apertures. For example, currently the collimators have a total aperture of 4 mm and the undulator vessels have a total aperture of 8 mm. Therefore, in the following it has been assumed that copper vessels have an aperture 4 mm and aluminium vessels have an aperture of 8 mm. The copper vessels are assumed to be in zero external magnetic field and the aluminium vessels in a field of 2 T.

A superconducting vessel based on the Diamond 3.5 T MPW has also been considered. The copper vessel has a 7 mm diameter, operates in a 3.5 T magnetic field and at a temperature of 4 K, a value of 60 for the RRR has been assumed. A circular vessel has also been assumed, although the wiggler vessel is elliptical.

### 4. Results

The power deposited in the vessel as a function of bunch length for the three different materials and two different surface resistivity models is shown in Figure 1 and Figure 2 for the HACL and XUV-FEL line respectively. A graph of the power for the

superconducting vessel is shown in Figure 3. A graph of the power per meter for increasing vessel radius is shown in Figure 4 for room temperature copper and aluminium type 6164.

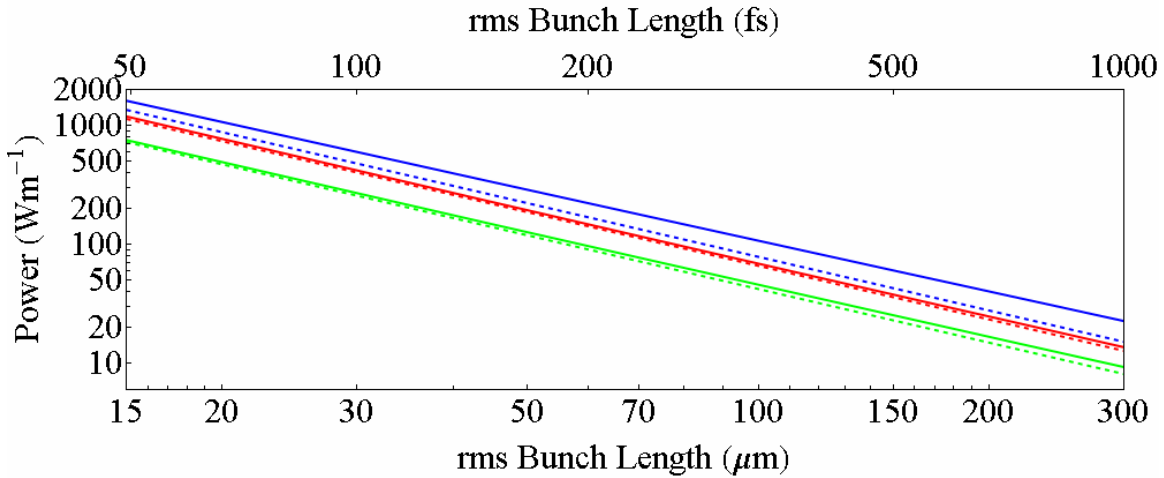


Figure 1: Power deposited in an 8 mm aperture aluminium (green), aluminium alloy (blue) and 4 mm aperture copper (red) vessel due to image current heating in the 4GLS HACL using the normal surface resistivity (solid lines) and the ASE surface resistivity (dashed lines) models.

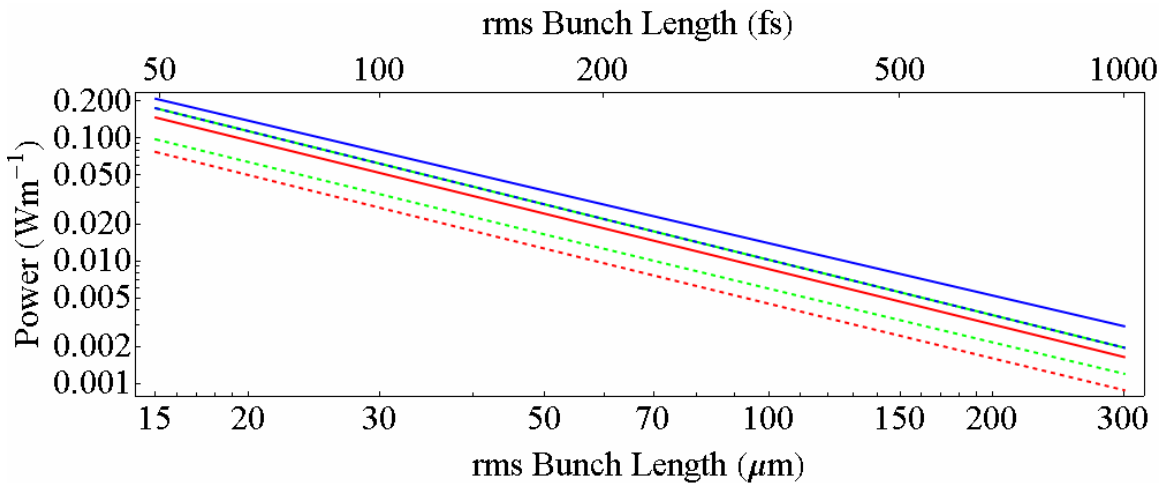


Figure 2: Power deposited per meter in an 8 mm aperture aluminium (green), aluminium alloy (blue) and 4 mm aperture copper (red) vessel due to image current heating in the 4GLS XUV-FEL line using the normal surface resistivity (solid lines) and the ASE surface resistivity (dashed lines) models.

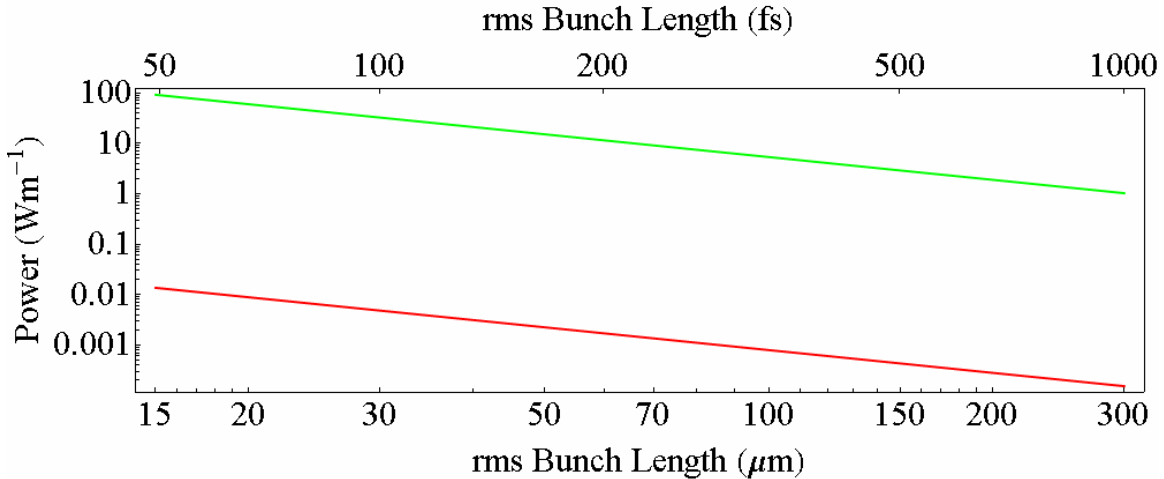


Figure 3: power deposited per meter in a 7 mm copper vessel with an RRR of 60 operating in a 3.5T magnetic field and at 4K for the HACL (green) and XUV-FEL line (red).

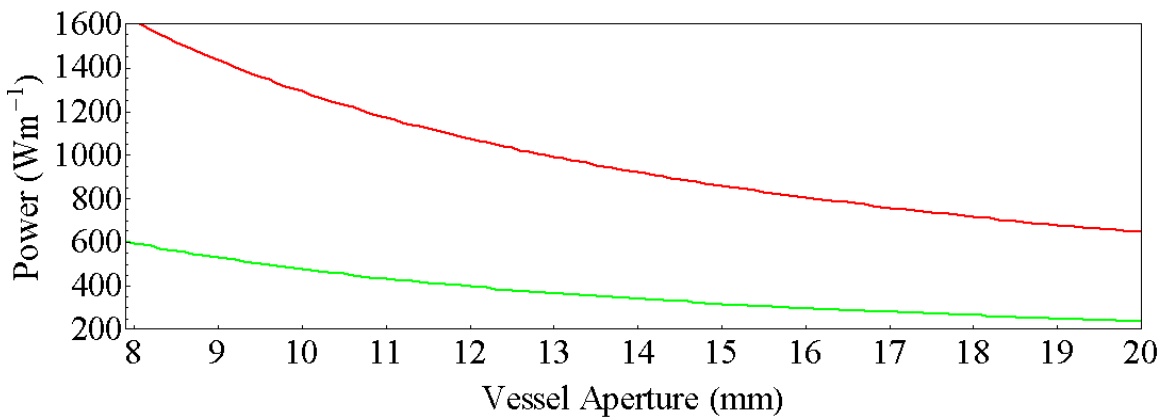


Figure 4: power deposited in a copper (green) and aluminium Type 6164 (red) vessel for increasing vessel aperture in the 4GLS HACL.

## 5. Comparison With Energy Lost due to Resistive Wall Wakefields

The energy lost by the beam due to resistive wall wakefields (RWW) should mostly be deposited in the vessel (some frequencies may propagate down the vessel) and therefore should be roughly equivalent to the image current heating. Resistive wall wakefields are explained in a number of places [11]. A comparison of the power lost in the HACL line for a copper and aluminium vessel is shown in Figure 5. There is a reasonable agreement between the two methods except for extremely short bunches and an aluminium vessel.

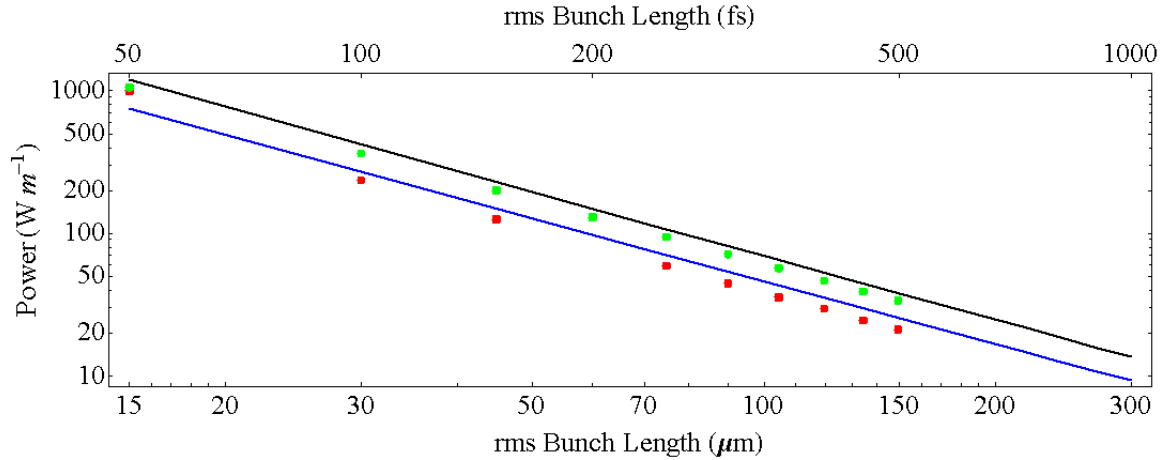


Figure 5: Power per m due to image current heating (lines) and lost by the beam due to the resistive wall wakefields (points) for an 8 mm aluminium vessel (blue, red) and a 4 mm copper vessel (black, green) .

## 6. Conclusions and Further Work

The heating of the vessel due to image currents has been estimated for copper, aluminium and aluminium alloy type 6164 and the 4GLS HACL and XUV-FEL line. Dissipated powers for sample bunch lengths for the copper and aluminium alloy vessels are given in Table 3.

Vessel	Vessel Radius (mm)	Field (T)	Bunch Length		Dissipated Power	
			(fs)	( $\mu m$ )	HACL	XUV
Copper	2	0	400	120	50	$6.8 \cdot 10^{-3}$
Al-Alloy (6164)	4	1	50	15	1614	0.21
Al-Alloy (6164)	4	1	100	30	600	$77 \cdot 10^{-3}$
Al-Alloy (6164)	4	1	500	150	60	$8 \cdot 10^{-3}$
Al-Alloy (6164)	4	1	1000	300	23	$3 \cdot 10^{-3}$

Table 3: Image current heating ( $W m^{-1}$ ) for copper collimator vessel and aluminium alloy undulator vessels for specific bunch lengths in the 4GLS HACL and XUV lines.

The theory outlined is for a circular vessel or two parallel plates of infinite extent. The vessels in 4GLS will most likely be elliptical and this will reduce any heating by a numerical factor of approximately 2 to 3. Also, the theory is for a Gaussian longitudinal bunch distribution and it is likely that this will not be the case. If, as is more probable, the charge distribution is “spiky” then the higher frequency components will induce more heating. Therefore it is only reasonable to consider the results as an estimate of the order of magnitude of the vessel heating.

Due to the  $I_0^2$  dependence and low average current of the XUV-FEL line the heating is not a significant issue. For the HACL line there could be  $\sim kW$  of power deposited for the shortest bunches and this has to be dissipated effectively so as to not

cause too much heating of the undulator magnets. Heating of permanent magnets would affect the magnetic performance of the undulator. Any cooling could decrease the total available magnetic gap by a few mm and this would change the undulator parameters required to meet the desired radiation output energy.

The energy spread increase is not considered here as the model only gives the time-averaged heating of the vessel. Although a copper vessel is heated less due to image currents aluminium was chosen in the 4GLS CDR because the associated wakefield damps differently and had less impact on the bunch energy spread, which must not be too high for the FEL operation [10]. The energy spread increase, and other resistive wall wakefield effects, from a more realistic bunch structures and improved models of the vessel conductivity will need to be looked at in future studies.

If a super-conducting wiggler such as the 3.5T wiggler from Diamond was to be used in the HACL there would be a severe limitation on the minimum bunch length that could be passed through it. For a 1m device the bunch length would have to be  $\sim 1000$  fs to not induce a quench, assuming a cooling power of  $\sim 10$ W, which also has to handle the power deposited in the vessel due to the synchrotron radiation produced in the wiggler and upstream elements. It seems likely that the image current heating effects would make incorporating any superconducting magnet on the 4GLS HACL difficult.

The current studies assume the beam and the vessels are perfectly aligned. Off-axis beams will cause more heating, for long bunches, by a factor of  $\left(\frac{b^2 + a^2}{b^2 - a^2}\right)$ , where  $b$  is the aperture and  $a$  is the displacement of the beam off-axis [12]. This would increase the heating by up to 20% for a mm off-axis beam.

No assessment of the temperature increase of the vessel has been made. The power will be deposited in a small volume of material and could therefore, especially in extreme cases, melt the vessel. (It must be remembered that the collimators must be designed to have a certain percentage of the beam impinge on them and so there could be a significant increase in the heating due to off-axis beams.) To further analyse this a detailed study of the failure modes of 4GLS, with more detailed information on the materials used and vessel and bunch geometry is required.

## 7. References

- 1 W.Chou and F. Ruggiero, “*Anomalous Skin Effect and Resistive Wall Heating*,” LHC Project Note 2 (SL/AP), 1995.
- 2 F. Caspers, M.Morvillo, and F.R. and J.Tan, “*Surface resistance measurements and estimate of the beam-induced resistive wall heating of the LHC dipole beam screen*,” Tech. Rep. LHC Project Report 307, CERN, 1999.

- 
- 3 S. Chouhan, R. Rossmanith, S. Strohmer, D. Doelling, A. Geisler, A. Hobl, and S.Kubsky, “*Field error compensation and thermal beam load in a superconductive undulator,*” in Proceedings of the 20th Particle Accelerator Conference, (Portland), 2003.
  - 4 E. Wallen and G. LeBlanc, “*Cryogenic system of the MAX-wiggler,*” *Cryogenics*, vol.44, pp.879-893, 2004.
  - 5 E. Wallen, J. Chavanne, and P.Elleaume, “*Magnetic calculations of a superconducting undulator at the ESRF,*” *Nucl. Instrum. Methods Phys. Res., Sect. A*, vol. 541, pp. 630-65093, 2005.
  - 6 S. Casalbuoni, M. Hagelstein, B. Kostka, R. Rossmanith, E. Steffens, M. Weisser, A. Bernhard, D. Wollmann, and T. Baumbach, “*Investigations of the thermal beam load of a superconducting in-vacuum undulator,*” in Proceedings of the 10th European Particle Accelerator Conference, (Edinburgh), 2006.
  - 7 E.Justi and M.Kohler, “*Über die elektrische leitfähigkeit der alkalimetalle im magnetfeld,*” *Annalen der Physik*, vol.428, no.3-4, pp.~349-356, 1939.
  - 8 G.E.H Reuter & E.H. Sondheimer “*The Theory of the Anomalous Skin Effect in Metals*” *Proc. Roy. Soc.Lond A*195, Pg336, 1949
  - 9 A.B. Pippard, *Proc. Roy. Soc.Lond A*191, Pg385, 1947
  - 10 4GLS Conceptual Design Report, 2006
  - 11 K. Bane and G. Stupakov, “*Resistive Wall Wakefield in the LCLS Undulator Beam Pipe,*” SLAC-PUB-10707, 2004
  - 12 A. Chao “*The Physics of Collective Beam Instabilities*” John Wiley and Sons, 1993.